Contents lists available at ScienceDirect

Nuclear Inst. and Methods in Physics Research, A

Characterization of a 2 × 2 array of large square bars of LaBr$_3$:Ce detectors with γ-rays up to 22.5 MeV

M. Dhibar [a], I. Mazumdar [b,*], P.B. Chavan [b], S.M. Patel [b], G. Anil Kumar [a]

[a] Department of Physics, Indian Institute of Technology Roorkee, Roorkee-247667, India
[b] Department of Nuclear and Atomic Physics, Tata Institute of Fundamental Research, Homi Bhabha Road, Colaba, Mumbai-400005, India

A B S T R A C T

LaBr$_3$:Ce scintillators have recently become commercially available in sizes large enough for measurements of high energy gamma-rays. In this communication, we report our studies on properties and response of large volume square bars ($2'' \times 2'' \times 8''$) of LaBr$_3$:Ce detectors, individually, and in a compact array of four square bars, with gamma-rays up to 22.5 MeV. The properties studied are, uniformity of the crystal, internal radioactivity, energy resolution, timing resolution, linearity of the response and detection efficiencies. The response of the detectors for 22.5 MeV γ-rays produced from ^{11}B$(p, \gamma)^{12}$C capture reaction and for 15.1 MeV γ-rays produced from ^{12}C$(p, p'\gamma)^{12}$C inelastic scattering reaction are studied in detail. The measured absolute efficiencies (both total detection and photo-peak) for 662 keV gamma-rays from ^{137}Cs are compared to those obtained using realistic GEANT4 simulations. The primary aim of the array is to measure high energy gamma-rays (5–50 MeV) produced from the de-excitation of excited Giant Dipole Resonance (GDR) states, radiative capture reactions, nuclear Bremsstrahlung process and inelastic scattering process. The highly satisfactory performance of the array provides the impetus for future efforts toward building a bigger array.

© 2017 Elsevier B.V. All rights reserved.

1. Introduction

The advent of lanthanum bromide scintillation detector has been a very important development in the field of gamma-ray spectroscopy. The much superior properties of this scintillator, compared to other existing scintillators, have resulted in increasing demand of these crystals and their in-depth characterizations [1]. The attractive features of Lanthanum Bromide (LaBr$_3$:Ce) scintillator, such as, better energy resolution [2], fast decay time [2,3], high detection efficiency [4], stability of light output with temperature [5] make it suitable in many applications that include medical imaging, nuclear spectroscopy, remote sensing, oil well logging, security, space, fusion plasma, environmental radioactivity, marine radioactivity monitoring, etc. [6–14]. In a recent publication [15] the authors have demonstrated the applicability of large volume LaBr$_3$:Ce detectors in experiments with relativistic beams and the reduction of Doppler broadening using position sensitive photo tubes coupled to such large volume LaBr$_3$:Ce detectors. Few individual groups and international collaborations have built arrays of LaBr$_3$:Ce detectors of different sizes and shapes. An overview of the use of arrays of small volume LaBr$_3$:Ce detectors (FATIMA [16], ROSPHERE [17],

NANA [18]) by combining with HPGe detectors for use in nuclear spectroscopy can be found in Ref. [19].

The spectroscopy of high energy gamma-rays (> 5 MeV) have traditionally been carried out by using either large volume NaI(Tl) or BaF$_2$ detectors or arrays of them [20–23]. The much superior properties of LaBr$_3$:Ce scintillators naturally lead to the demand for growing them in bigger volumes for efficient detection of high energy gamma-rays. The better energy resolution and faster timing of LaBr$_3$:Ce would result in superior quality spectra and better neutron-gamma separation. The better energy spectrum would show clear separation of photo-peak and escape peaks for high energy gamma rays which is not the case for NaI(Tl) and BaF$_2$ detectors. It is by now well established that large volume LaBr$_3$:Ce detectors certainly provide better choice over the time tested NaI(Tl) and BaF$_2$ detectors in many applications.

In recent years different groups have reported characterization of large volume single Lanthanum Bromide crystals. Mazumdar et al. have reported the measurement of response of a large volume cylindrical LaBr$_3$:Ce crystal up to 22.5 MeV monochromatic gamma-rays [24]. Naqvi et al. have studied the properties and response of $4'' \times 4''$ LaBr$_3$:Ce crystal up to 10 MeV gamma rays [25]. Giaz et al. have reported the

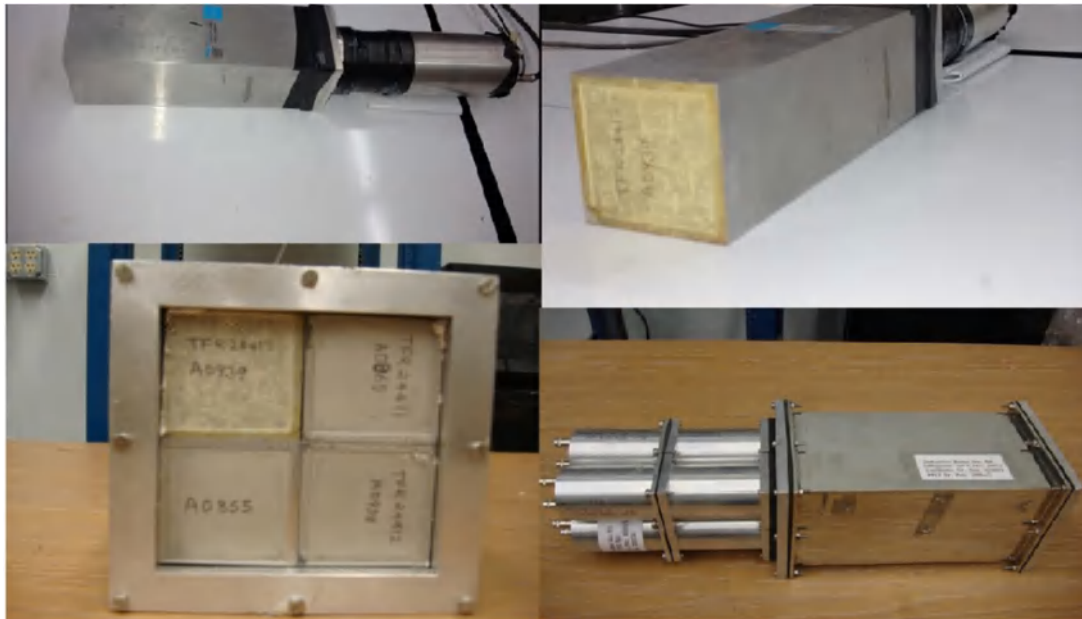**Fig. 1.** Photographs of the large volume square bars of LaBr$_3$:Ce detectors (single crystals and compact array of four square bars).

measurement of response of a $3.5'' \times 8''$ LaBr$_3$:Ce crystal up to 22.5 MeV gamma-rays [26]. The measurements of high energy gamma-rays from GDR and nuclear Bremsstrahlung processes and measurements of gamma strength functions are being explored by PARIS and HECTOR$^+$ arrays [27–30]. To the best of our knowledge no data on response of an array of large volume LaBr$_3$:Ce detectors with high energy gamma rays, say, in the range of 15–30 MeV has been reported so far. In the present work, we report our studies on properties and response of large volume square bars of LaBr$_3$:Ce detectors ($2'' \times 2'' \times 8''$), individually, and in a compact array of four bars for high energy gamma- rays up to 22.5 MeV. We have also carried out detailed realistic simulations to generate the response of these detectors to gamma-rays using GEANT4 toolkit [31]. The primary motivation behind characterizing these detectors is to build an array of large volume LaBr$_3$:Ce detectors for efficient measurement of gamma-rays up to 50 MeV. Such an array will be highly useful for studying GDR decay, nuclear Bremsstrahlung, radiative capture reactions and inelastic scattering reactions. Unlike scintillators like NaI(Tl), Lanthanum Bromide crystals are very difficult to grow in large volumes and in different shapes. Since the efficient measurement of high energy gamma-rays demand larger volumes, one obvious solution is to build compact arrays of smaller volume detectors. To this end, we have decided to build an array of square bars of LaBr$_3$:Ce detectors. Such an array can be built up to any size (volume) depending upon the experimental requirement and the availability of funds. The array to be discussed in this paper is built of large volume square bars of LaBr$_3$:Ce detectors. This paper is organized as follows. Section 2 describes the design of the individual detectors and the array and associated electronics. In Section 3, we will discuss the measurements to study the various properties of the detectors, namely, uniformity and homogeneity of the crystal, internal radioactivity, energy resolution and timing resolution. This section also covers linearity of response of the single crystals and the compact array to gamma-rays from calibrated radioactive sources and in-beam nuclear reactions. Section 4 discusses the GEANT4 simulations and efficiency calculations. Section 5 presents the summary.

2. Detector assembly and associated electronics

Fig. 1 presents the photos of the large volume square bars of LaBr$_3$:Ce detectors, (single crystals and compact array of four square bars) used

in the measurements. Each detector has a dimension of $2'' \times 2'' \times 8''$. The combined volume of the array of four such crystals is more than double the volume of a $3.5''$ diameter and $6''$ long LaBr$_3$:Ce cylinder that we have earlier studied and reported about [24]. The crystals were manufactured and supplied by Saint Gobain Inc. [1]. Each crystal is encased in 2 mm thick Al housing with one end along the length, fitted with a glass window. The space between the crystal surface and the Al casing is packed with 5 mm thick reflecting material.

As has been discussed in our previous publications [7,24] the best performance of LaBr$_3$:Ce vis-à-vis energy or timing resolution is governed by judicious choice of the photomultiplier tube (PMT). We have tested performance of LaBr$_3$:Ce detectors with a variety of PMTs and have zeroed upon ET 9266B tubes for extracting the best performance for gamma-ray spectroscopy. These tubes have bialkali photocathodes and the dynode structures have ten stages. The maximum anode dark current is 1.5 nA and the rise time of the anode pulse is 4 ns. The electron transit time is 40 ns. The spectral response of the ET 9266B tubes range from 290 to 630 nm with a maximum value at ~360 nm. We have coupled each of the square bar detectors to $2''$ diameter ET 9266B PMT. The home-made PMT base houses both the voltage divider and a charge sensitive preamplifier. The gain stabilization at high count rate is taken care of by transistors in the last four stages of the voltage divider. The energy and timing signals are drawn from one of the dynodes and the anode respectively. The preamplifier uses J-FET input operational amplifier LF351 and NPN/PNP transistors at the output stage. The rise time of the preamplifier output pulse is less than 100 ns and the fall time is less than 100 μs. The designs of the voltage divider and the preamplifier have been described in detail in a previous publication [24] and will not be discussed here any further. A rectangular Al structure with suitable flanges was designed to house the compact array of the four square bars (Fig. 1). Some of the major details of the PMT are given in Table 1.

3. Characterization of detectors with calibrated γ-sources

The major properties of the large volume square bars of LaBr$_3$:Ce detectors, individually, and in a compact array of four square bars, have been studied using calibrated γ-sources, namely, ^{137}Cs (661.6 keV), ^{60}Co (1173 keV, 1332 keV), ^{133}Ba (303 keV, 356 keV), ^{22}Na (511 keV, 1274 keV) and ^{241}Am- ^{9}Be (4433 keV). The properties studied

Table 1
Specification of the PMT used in our measurements.

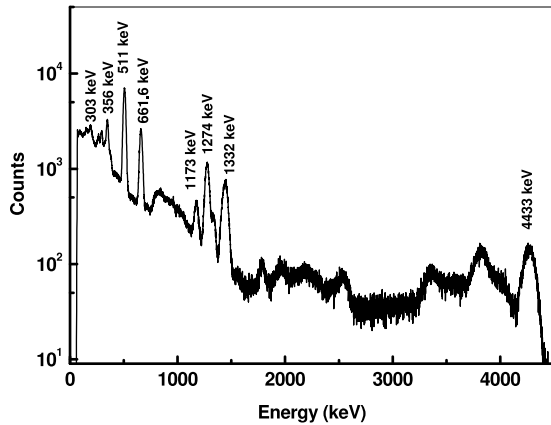| Model	ET9266B, ET enterprises
Diameter	51 mm (Active 48 mm)
Quantum efficiency	30%
Window material	Borosilicate
Number of Dynodes	10 stages
Spectral range	290 to 630 nm
Transit time	40 ns
Typical cathode to anode operating voltage	850 V

Fig. 2. Typical spectrum recorded with a single square bar using different γ-sources.

Fig. 3. Plot of energy versus pulse height for the single square bar at different voltages for four different γ-ray energies.

Fig. 4. Linear response of the square bar for nine different energies up to 4.433 MeV at −450 V. The plot of ($E_{real} - E_{measured}$) vs E_{real} has been shown in the inset.

are uniformity and homogeneity, internal radioactivity, linearity of the response, energy resolution and timing resolution. Fig. 2 shows a typical spectrum recorded with a single square bar of LaBr$_3$:Ce using all the γ-sources mentioned above. The detector well resolves the close lying peaks of ^{133}Ba (303 and 356 keV) and ^{60}Co and ^{22}Na (1173, 1275 and 1332 keV). Evidently, time tested scintillators like NaI(Tl) or BaF$_2$ have much worse energy resolutions and cannot produce such spectra resolving all the lines. Similar performance by a small volume (13 cm^3) cylindrical (1″ × 1″) LaBr$_3$:Ce detector and a large volume (946 cm^3) cylindrical (3.5″ × 6″) LaBr$_3$:Ce detector reported by us can be found in Ref. [7,24].

3.1. Linearity & energy resolution up to 4.433 MeV

The excellent energy resolution of LaBr$_3$:Ce is mostly due to the very high light output of about 61000 photons/MeV [2]. However, this high light yield produces high surge of current in the PMT at higher energies (>1 MeV) leading to non-linear response. The non-linearity can be very severe at higher gamma energies. As the primary objective of the array is to measure the high energy gamma-rays and to attain larger dynamic range (say up to 40 MeV) of operation, it is imperative to tackle the problem of non-linear response with increasing gamma-ray energy. In order to determine the optimum operating conditions that ensure a linear response the measurements were carried out using radioactive sources emitting gammas in the energy range of 661.6 keV to 4.433 MeV. In addition, we have performed proton induced reactions to produce high energy, monochromatic gamma-rays of 15.1 and 22.5 MeV. We first discuss the measurements with the radioactive sources. The in-beam measurements will be presented in a later sub-section. The optimum performance of the detector regarding linearity, energy and timing resolutions is determined by the right choice of the PMT, the operating voltage and drawing the energy signal from a lower dynode. It has been discussed in our previous publications [7,24] that a specific combination of operating voltage and lower dynode provides a linear response over the range of interest for a given dynamic range. The attainment of linearity up to a certain energy range comes at the cost
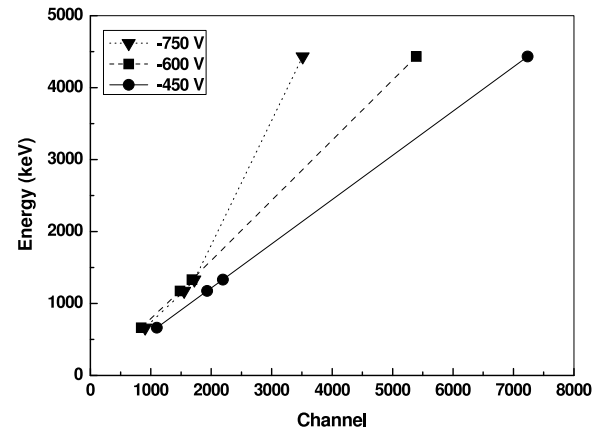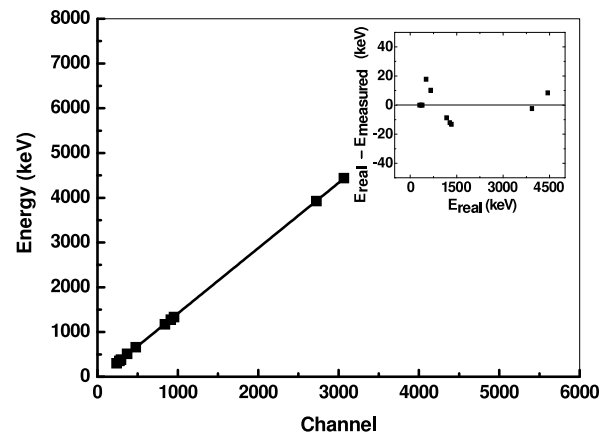
of reduced energy resolution. While the best energy resolution for a detector is obtained by operating the PMT at a higher voltage and drawing the signal from the anode, the linearity was found to be better, as expected, when energy signals are taken from a lower dynode. As the choice of specific dynode and operating voltage depends on the range of energy of interest, we have recorded the energy spectra for signals drawn from fourth dynode onwards and changing the operating voltage was from −450 to −800 V. Fig. 3 shows, for the single square bar, the plot of energy versus pulse height for different values of operating voltage while drawing the energy signal from the second last dynode. Clearly, the signals tend to become highly non-linear with gamma-ray energy for higher operating voltages. A perfectly linear response is obtained up to 4.433 MeV for an operating voltage of −450 V for the ET 9266B tubes. Fig. 4 shows the excellent linear response for a square bar when tested with several gamma-ray sources from 661.6 keV (^{137}Cs) to 4.433 MeV (AmBe). We also show the variation and its spread in the values in the inset of Fig. 4 by plotting ($E_{real} - E_{measured}$) vs E_{real}.

The energy resolutions were also measured for different combinations of operating voltage and dynode for the ET 9266B PMTs. As mentioned earlier and discussed in [7,24] the energy resolutions worsen with decreasing operating voltage and lower dynode. Fig. 5 shows the plots of resolution versus gamma energy for three different operating voltages, namely, −450, −600 and −750 Volts for the full array of four closely packed square bars of LaBr$_3$:Ce detectors. Clearly the energy resolutions deteriorate with decreasing bias voltage for a fixed energy. Our plot shows that for the array, the best energy resolution obtained is ~4.3% for 661.6 keV at −750V. This is almost same for the single

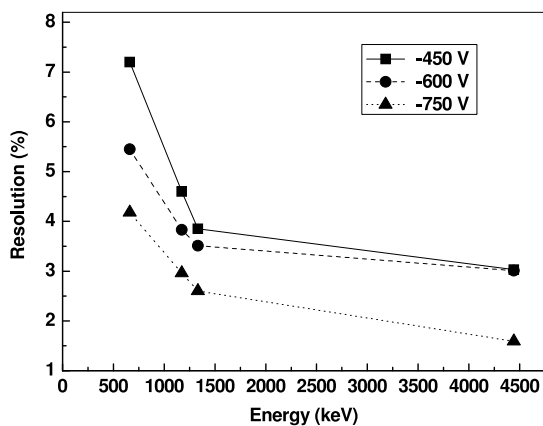**Fig. 5.** Resolution versus Energy plot of the array for different operating voltages.

Fig. 7. Dynamic ranges of single square bar and the full array measured with cosmic ray muons.
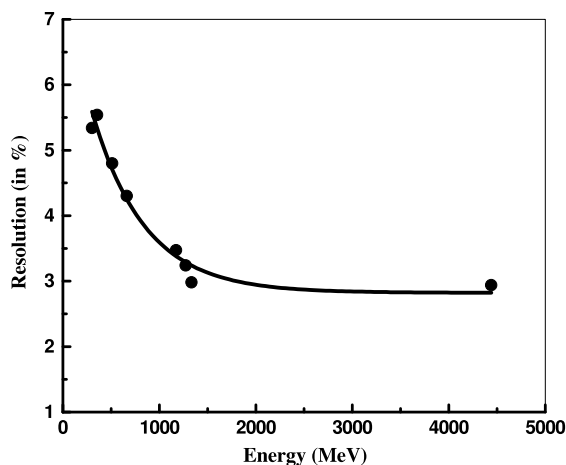

Fig. 6. Resolution versus Energy plot for the array measured at eight different energies up to 4.433 MeV. The solid line is a fit showing the typical $1/\sqrt{E}$ dependence.

square bar operated at −750 volts. At the highest bias voltage of −750 V the energy resolution is 1.6% at 4.433 MeV. While the resolutions at lower voltages (−450 and −600 Volt) also improve and become almost 3% at 4.433 MeV. Fig. 6 shows the resolution vs energy plot for the array measured at eight different energies up to 4.433 MeV along with the fitted function showing the typical $1/\sqrt{E}$ dependence.

3.2. Dynamic range of the array and a single detector

As mentioned before the primary aim of setting up this array of large volume detectors is to measure high energy gamma-rays, say, up to 50 MeV. One would therefore be interested to know about the dynamic range of the single detector and the full array. This is achieved by measuring the background cosmic ray spectrum. The cosmic rays at sea level are predominantly high energy muons. The relativistic muons passing through the detector material loses energy at a fixed rate per unit travel path. The value of the energy loss (dE/dx) depends upon the elemental composition of the crystal. Fig. 7 depicts the dynamic range of both single square bar and the full array. Both the spectra show the characteristic peaks near the end of the spectra. The maximum energy deposited in the single crystal is around 40 MeV and, for the array it can go up to 80 MeV. For a large cylindrical LaBr$_3$:Ce of length 6″ and diameter 3.5″ [24] we have measured the dynamic range to be around 35 MeV.

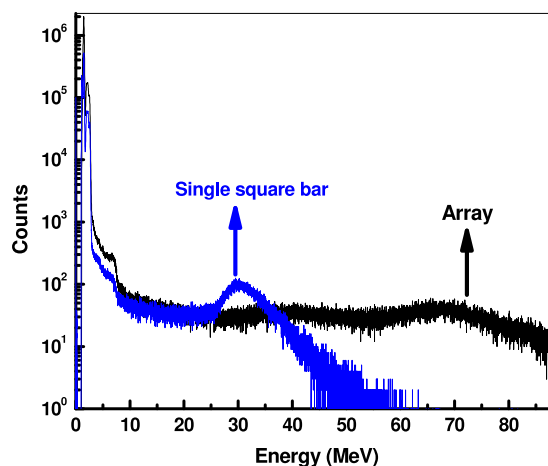### 3.3. Homogeneity and uniformity

One of the major challenges faced by the crystal grower is to produce a defect-free single crystal that is uniform in its response irrespective of the region of interaction with radiation in the detector volume. The difficulty is even more acute for growing large volume LaBr$_3$:Ce crystals which has relatively weak (100) cleavage plane and hexagonal crystal structure with considerable anisotropy in properties, like thermal expansion. It is, therefore, essential to check the homogeneity and uniformity of a large volume LaBr$_3$:Ce crystal to confirm the presence of any structural defect. To investigate this, the measurements were carried out using two collimated γ-sources namely, ^{137}Cs (661.6 keV) and ^{60}Co (1173 keV, 1332 keV). The pulse height measurements were done by changing the position of the sources along the length of the detector for all the four sides. The γ-rays coming from ^{60}Co probe deeper inside the crystal volume than the γ-rays coming from ^{137}Cs. Fig. 8(a) presents the variation of pulse height along the length of the crystal for all the four sides for all three gamma energies (661.6, 1173, 1332 keV). The observation is that the pulse height is almost same along the length of the crystal and doesn't change by more than a percent from end to end. There is very nominal change in the pulse height for the different sides. The uncertainty associated with the pulse height measurements are found to be within ±1%. The response of the crystal can safely be considered as uniform and highly satisfactory. The results are very similar to what was reported earlier for a large volume cylindrical crystal of LaBr$_3$:Ce [24]. In order to show the variation in pulse height and its spread from the average value, that is not visible in the plot 8a, we show in Fig. 8(b) the spread in the deviation from average pulse height along the length for three different γ-rays energies for one of the four surfaces.

3.4. Internal radioactivity

Notwithstanding the many superior qualities of LaBr$_3$:Ce it still has a few drawbacks, namely, difficulty in growing large crystals and presence of internal radioactivity. The internal activity spectrum of LaBr$_3$:Ce crystal is due to α, β and γ emission from few tens of keV to nearly 3 MeV. The self-activity up to ∼1.6 MeV is primarily due to β and γ- decay from ^{138}La and the triple peak structure beyond 1.6 MeV is mainly due to the α decay of ^{227}Ac and their daughter nuclei. A more detailed discussion on internal activities of LaBr$_3$:Ce is provided in [24]. The internal radioactivity LaBr$_3$:Ce detector is a major drawback in low background applications limiting its applications to low count rate experiments. Several authors have investigated the internal activities of LaBr$_3$:Ce and there exists considerable literature on the subject [4,32,33]. Giaz

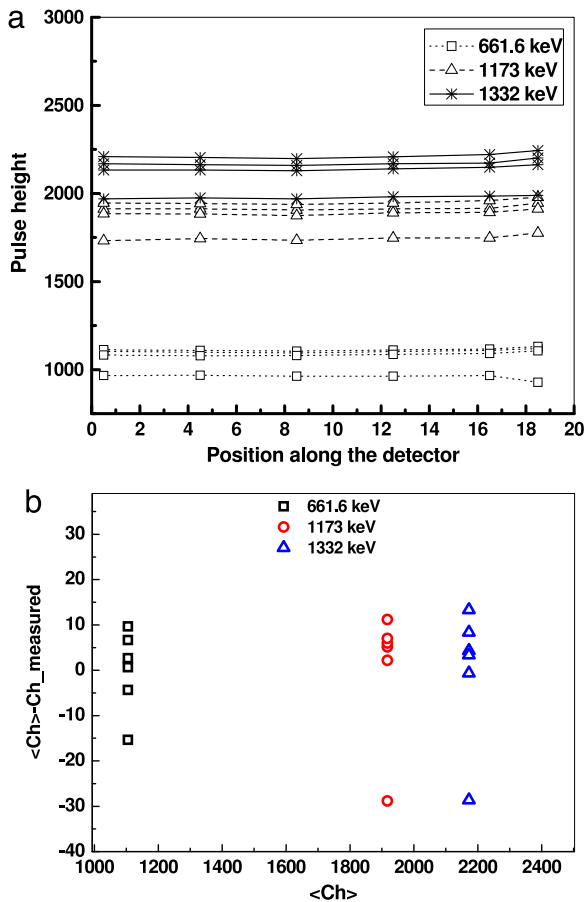**Fig. 9.** Background spectrum recorded in the array with and without the shielding.

Fig. 8. (a) Variation of pulse height along the length of the single square bar for all the four sides measured at three different γ-ray energies. (b) The spread in the deviation from average pulse height along the length for three different γ-rays energies.

et al., [34] have made detailed measurements on internal radioactivity of LaBr$_3$:Ce detector in order to study the characteristics of beta decay and have explored the possibility of reducing the natural background below 789 keV. Very recently, Wolszczak and Dorenbos [35] have shown the important role of nuclear gamma de-excitations on the shape of the internal alpha spectrum measured in scintillators. In the past, we have tested a phoswich detector composed of $3'' \times 0.5''$ LaBr$_3$:Ce with $3'' \times 1''$ NaI(Tl) and have reported a significant reduction in the general background and about 20% reduction in the X-ray peak due to internal activity near 30 keV [36]. In the present work, we have measured the count rate of internal activity by completely shielding the entire detector assembly with 6 in. thick layers of Lead. Fig. 9 shows the background spectrum recorded in the compact array of four square bars of LaBr$_3$:Ce detectors with and without the shielding. The prominent peak at around 1.5 MeV region is due to the presence of many γ-rays, namely, 1.436 MeV γ-ray from ^{138}Ba (populated by electron capture of ^{138}La), 1.468 MeV γ-ray due to the summing of 1.436 MeV and 32 keV X-ray from ^{138}La and 1.46 MeV γ-rays from naturally occurring ^{40}K present in the surroundings. The triple peak structure is due to the α decay of ^{227}Ac to the daughter nuclei namely, ^{227}Th, ^{223}Ra, ^{221}Bi, ^{219}Rn and ^{215}Po. The energy and the branching ratios of the α peaks are discussed in detail in Ref. [4,32]. The recorded spectra shown in Fig. 9 is due to contributions from both internal activity of the detector and external terrestrial radiation. The shielding suppresses the external activity up to around 800 keV. The shielded spectrum is almost entirely due to the internal activity. The count rate of internal activity in the array is estimated to be 1.02 cts/s/cm^3.
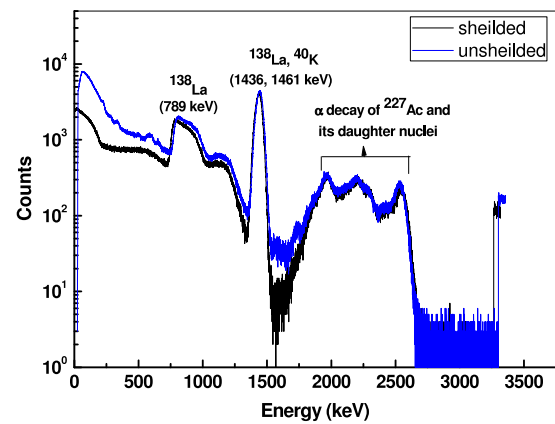
3.5. Response to high energy gamma rays and linearity up to 22.5 MeV

Our primary motivation behind building the array of large square bars of LaBr$_3$:Ce detectors is measurement of high energy gamma-rays up to ~50 MeV. The analysis of the continuum gamma-ray spectrum, say, from the decay of GDR states in hot and rotating nuclei, demands complete understanding of the response of the array for high energy gamma rays. The two common radioactive sources to produce high energy gamma-rays are ^{241}Am- ^{9}Be (4.433 MeV) and ^{244}Cm- ^{13}C (6.13 MeV). These sources are combinations of alpha emitters and stable isotopes populating the first excited states of ^{12}C (4.433 MeV) and ^{16}O (6.13 MeV). In-beam experiments are required to generate high energy monochromatic γ-rays beyond 6.13 MeV. These in-beam experiments are based on either inelastic scattering or proton capture processes. Few in-beam reactions have been reported so far to study the response of medium and large volume LaBr$_3$:Ce detectors to high energy gamma-rays (>10 MeV) [24,37,38]. To the best of our knowledge, only a few nuclear physics measurements have been reported so far using multiple large volume LaBr$_3$:Ce detectors [29,30,39]. We have carried out following two in-beam experiments to study the response of the compact array of four large volume square bars of LaBr$_3$:Ce detectors to high energy gamma-rays, of 15.1 and 22.5 MeV.

(1) The ^{11}B(p,γ)^{12}C capture reaction producing 22.5 MeV gamma-rays.
(2) Inelastic scattering of high energy protons off ^{12}C to produce 15.1 MeV gamma-rays.

It is to be noted that the energies of gammas produced in these two reactions are in the energy range of gammas produced from GDR decay of medium and heavy mass nuclei. Both the measurements were carried out at the 14 MV Pelletron accelerator facility in TIFR, Mumbai. The LaBr$_3$:Ce array (Fig. 1) was placed at a distance of 35 cm from the target position and at an angle of 90° with respect to the beam direction. Each of the four energy signals was drawn from the 8th stage of the dynode chain and the PMTs were operated at −450 Volts. All the four energy signals were gain matched and added passively in a linear adder. The four anode signals were ORed to provide the timing signal. The necessary details of the in-beam reactions are listed in Table 2.
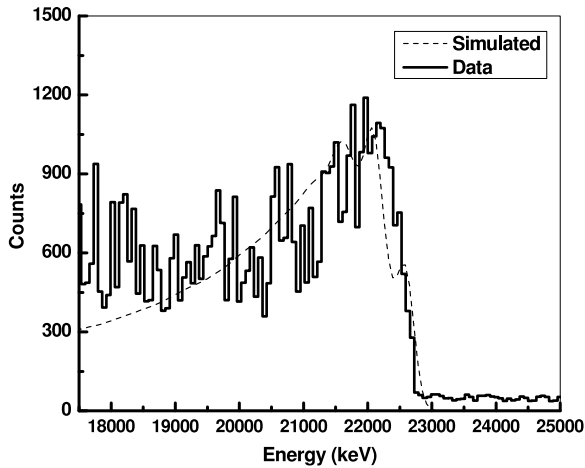
Fig. 10 shows the energy spectrum measured in the array for 22.5 MeV gamma rays produced from the capture reaction of ^{11}B(p,γ)^{12}C. Here, the photo-peak is much less dominant than the 1st escape peak due to the relatively small volume of the array for the rather high energy gamma-rays of 22.5 MeV. The solid line is the GEANT4 reproduction of the spectral shape for 22.5 MeV gamma-rays impinging upon the detector array. Prior to the GEANT4 simulation the data was fitted to extract an energy resolution of 1.2% for 22.5 MeV γ−rays. This value

Table 2
Details of the in-beam reactions used to produce high energy gamma rays.

Reaction	Target (Thickness)	E_p (MeV)	Q (MeV)	E_γ (MeV)	I (nA)
^{11}B(p,γ) ^{12}C	^{11}B (1 mg/cm^2)	7.2	15.957	22.5	7
^{12}C(p,p′γ)^{12}C	Mylar (2.23 mg/cm^2)	19.5	−15.1	15.1	10

Fig. 10. Energy spectrum measured in the array for 22.5 MeV gamma rays produced from the capture reaction of ^{11}B(p,γ) ^{12}C.
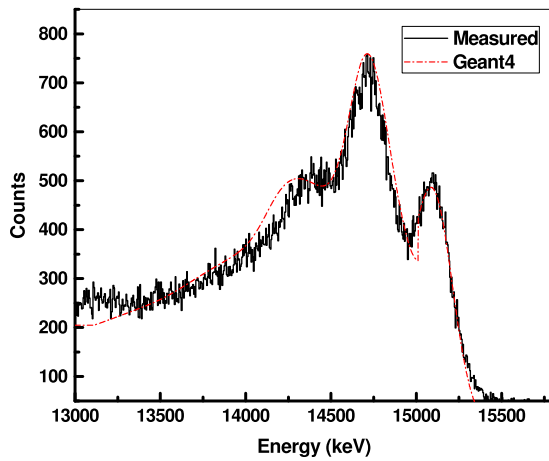

Fig. 11. Energy spectrum for 15.1 gamma rays produced in the inelastic scattering of protons off ^{12}C nucleus.

Fig. 12. Plot of pulse height vs energy for the array up to 22.5 MeV. The plot of $(E_{real} - E_{measured})$ vs E_{real} has been shown is the inset at −450 V.

is close to what we have reported earlier about the energy resolution of a large volume (946 cm^3) cylindrical (3.5″ × 6″) LaBr$_3$:Ce detector at 22.5 MeV [24]. The experimental resolution was used to generate the final simulated spectral shape for the 22.5 MeV gamma-rays (solid line in Fig. 10). Fig. 11 shows the energy spectrum for 15.1 gamma rays produced in the inelastic scattering of 19.5 MeV protons off ^{12}C nucleus. Owning to the much lower energy the array records a prominent photo-peak than what was observed for the 22.5 MeV gamma-rays. The solid line in Fig. 11 is the GEANT4 reproduction of the spectral shape for 15.1 MeV gamma-rays. Clearly there are advantages of using inelastic scattering reaction of ^{12}C(p, p′γ) ^{12}C over ^{11}B(p, γ) ^{12}C capture reaction. They are, (a) much higher cross section of production for the 15.1 MeV gamma-rays and consequently a much shorter beam time, (b) Mylar target is easily available compared to the rather non-trivial process of making thick boron target and (c) the 19.5 MeV proton beam is more easily delivered by a medium energy accelerator like Pelletron than 7.2 MeV protons required for the capture reaction.

Fig. 12 presents the pulse height vs energy plot for the array over the entire region from 662 keV to 22.5 MeV. The excellent linear response
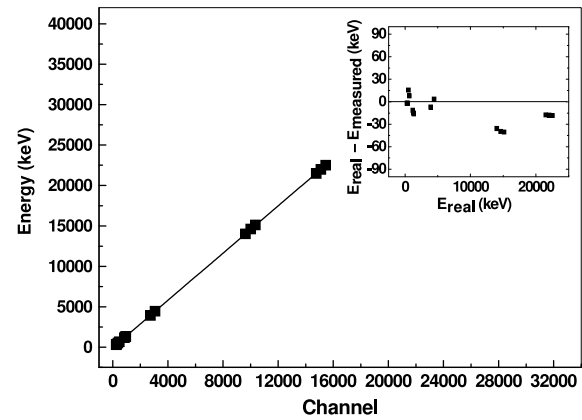
of the array is highly encouraging and ensures the meaningful use of array for high energy continuum gamma-ray spectroscopy.

3.6. Time resolution

The fast decay time of 30 ± 5 ns [2] offers a time resolution of about a few hundred picoseconds for LaBr$_3$:Ce making it an attractive scintillator for nuclear spectroscopy [4,7]. We have made timing measurements of the single square bar and of the array separately employing a standard slow fast coincidence circuit using ^{60}Co source. The coincidence measurements were performed using three different setups, namely, (1) two large square bars, (2) one square bar and a small cylindrical (1″ × 1″) LaBr$_3$:Ce and (3) one square bar and the full array of four square bars. For measurements of 1&2 the timing signals from the anodes were processed through CFDs and then fed to a Time-to-Amplitude Converter (TAC). The energy signals from the dynodes were processed through spectroscopic amplifiers and single channel analyzers (SCA) to produce energy windows of around 1 to 1.5 MeV including both the lines of ^{60}Co. The SCA outputs were ANDed and used to gate the TAC. For the coincidence between the array and a single bar the timing signals from the four detectors of the array were time matched and ORed to produce one of the inputs in the TAC. Fig. 13 shows the energy gated time spectra recorded using LaBr$_3$:Ce detectors of different sizes. For array vs bar and array vs 1″ cylinder, the FWHM values are found to be about 990 ps and 730 ps, respectively. In comparison, the smaller volume detectors show much better timing resolutions. We have earlier reported time resolutions of 235 ps and 650 ps for LaBr$_3$:Ce detectors of sizes 1″ × 1″ and 3.5″ × 6″ [7,24] respectively. The relatively worse time resolution in the present case is attributed to the larger volumes of the detectors involved. It is to be noted that one particular PMT cannot provide best energy resolution and time resolution at the same time. The present measurement is carried out with the ET 9266B PMTs. We expect much better timing if one uses faster PMTs like ET 9807B [7]. Nonetheless, the timing response studied for the single square bar and of the array is far superior than NaI(Tl) detectors of equivalent volumes and comparable to BaF$_2$.

4. Geant4 simulations and efficiency calculations

In order to understand the dependence of detection efficiency of the array on gamma energy and to create the energy dependent response matrix of the array, we have carried out extensive, Monte Carlo
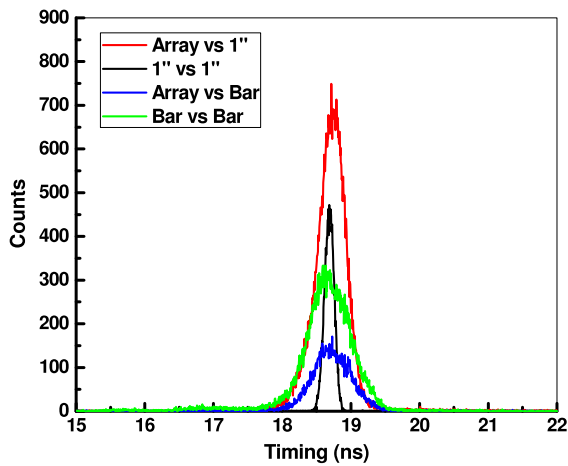
Fig. 13. Energy gated time spectra recorded using LaBr$_3$:Ce detectors of different sizes.

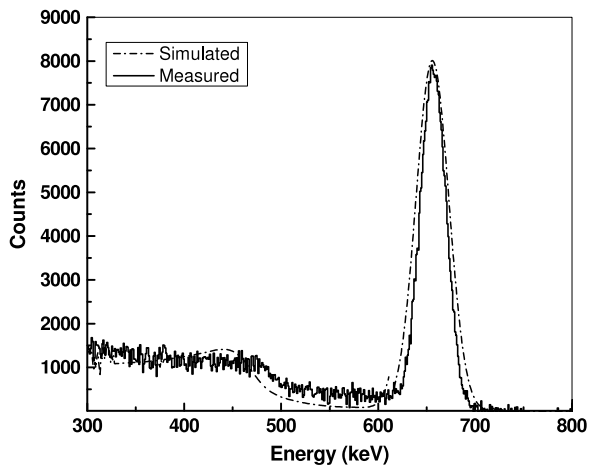**Fig. 14.** Gamma spectrum for 661.6 keV measured with the array along with the GEANT simulation (dashed-dotted line).

Table 3
The measured and simulated photo-peak efficiencies of the single square bar and of the array for 661.6 keV.

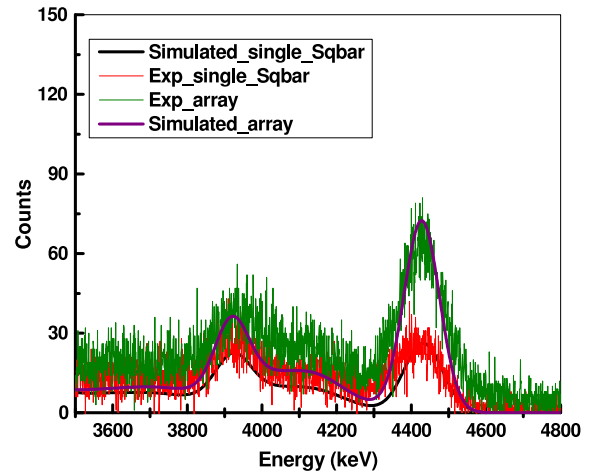| Detector geometry	Efficiency (%)	
	Experimental	Simulated
Single square bar	34.88 (0.03)	34.13 (0.05)
Array	40.50 (0.15)	41.00 (0.11)

Fig. 15. Response of the array and of the single square bar for 4.433 MeV gamma-rays. The solid lines are the outputs of GEANT4 simulations.

square bar for 4.433 MeV gamma-rays. The solid lines are the outputs of GEANT4 simulations.

5. Summary

In this paper, we have presented complete characterization of the large volume square bars of LaBr$_3$:Ce detectors, individually, and in a compact array of four square bars in 2×2 geometry. The response to gamma-rays was studied using radioactive sources and in-beam reactions. High energy monochromatic gamma-rays of 15.1 and 22.5 MeV were produced via inelastic scattering of 19.5 MeV protons off ^{12}C target and capture reaction of 7.2 MeV protons on ^{11}B target, respectively. An excellent linear response was obtained from 661.6 keV to 22.5 MeV for the complete array and individual single detectors by drawing the signals from lower dynode with operating voltage of −450V. The gamma-ray spectra from the sources and also for the 15.1 MeV and 22.5 MeV photons were reproduced using realistic GEANT4 simulations. The experimental efficiencies for 662 keV were found to be in very good agreement with the simulated ones. The detection facility would be ideal for spectroscopy of high energy (5–40 MeV) gamma-rays from GDR decay studies, capture reactions, nuclear Bremsstrahlung processes etc. A bigger square array of these LaBr$_3$:Ce detectors is presently being planned and will be reported on completion in future.

simulations for gamma energies from 661.6 keV to 22.5 MeV. The simulations were performed using the GEANT4 simulation toolkit [31]. The realistic simulations incorporated the details of detector geometry and the Aluminum housing of the detector using the data provided by the manufacturer. The Geant4 EM module and physics-lists [40,41] of the gamma interaction were used inside the simulation package to generate the gamma response of the detector. General particle source and radioactive decay module [42] was included inside the toolkit to simulate the gamma sources used during the experiment. The simulation was done by considering the isotropic emission of the point gamma source, by keeping the same target-to-detector separation value used in the experiment. The statistical uncertainties associated with full energy peaks due to the Monte Carlo nature of the simulations is found to be negligible because of very large number (about 10^6) of events considered in the simulations. Fig. 14 shows the gamma spectrum for 661.6 keV measured with the array along with the GEANT simulation (dashed-dotted line). The measured and simulated photo-peak efficiencies of the single square bar and of the array for 661.6 keV are summarized in Table 3.

The measured and simulated efficiencies are in very good agreement with each other. The add-back of signals from the four detectors in the array is expected to improve the photo-peak efficiency over a single square bar. This was tested for 4.433 MeV gamma-rays from an AmBe source. Fig. 15 shows the spectra recorded in the array and a single

References

[1] Please see http://www.crystals.saint-gobain.com/products/brillance-labr3-lanthanum-bromide for a detailed list of relevant references.
[2] P. Dorenbos, et al., IEEE Trans. Nucl. Sci. NS-51 (3) (2004) 1289.

[3] K.S. Shah, et al., IEEE Trans. Nucl. Sci. NS-50 (6) (2003) 2410.
[4] R. Nicolini, et al., Nucl. Instrum. Methods A 582 (2007) 554.
[5] M. Moszynski, et al., Nucl. Instrum. Methods A 568 (2006) 739.
[6] R. Pani, et al., Nucl. Instrum. Methods A 787 (2015) 46.
[7] G. Anil Kumar, et al., Nucl. Instrum. Methods A 610 (2009).
[8] Kozyrev, et al., Rev. Sci. Instrum. 87 (2016) 085112.
[9] G. Bizarri, et al., Phys. Status Solidi A 203 (2016) R41.
[10] F. Quarati, et al., Nucl. Instrum. Methods A 574 (2007) 115.
[11] I.G. Mitrofanov, et al., Planet. Space Sci. 58 (2010) 116.
[12] D. Riganonti, et al., Rev. Sci. Instrum. 87 (2016) 11E717.
[13] K. Ceupek, J. Radioanal, et al., Nucl. Chem. 299 (2014) 1345.
[14] Z. Zeng, et al., Appl. Rad. Isot. 121 (2017) 101.
[15] Blasi, et al., Nucl. Instrum. Methods A 839 (2016) 23.
[16] Regis, et al., Nucl. Instrum. Methods A 763 (2014) 210.
[17] Bucurescu, et al., Nucl. Instrum. Methods A 837 (2016) 1.
[18] G. Lorusso, et al., Appl. Rad. Isot. 109 (2016) 507.
[19] P.H. Regan, et al., J. Phys. Conf. Ser. 763 (2016) 012004.
[20] I. Mazumdar, et al., Nucl. Instrum. Methods A 417 (1998) 297 and references therein.
[21] Rathi, et al., Nucl. Instrum. Methods A 482 (2002) 355.
[22] Y.K. Agarwal, et al., Pramana-J. Phys. 35 (1990) 49.
[23] Takeuchi, et al., Nucl. Instrum. Methods A 763 (2014) 596.
[24] I. Mazumdar, et al., Nucl. Instrum. Methods A 705 (2013) 85.
[25] A.A. Naqvi, et al., Appl. Rad. Isot. 104 (2015) 224.
[26] A. Giaz, et al., Nucl. Instrum. Methods A 729 (2013) 910.
[27] A. Maj, et al., The Paris project, Acta Phys. Pol. B 40 (2009) 565.
[28] Ceruti, et al., Phys. Rev. C 95 (2017) 014312.
[29] Larsen, et al., Phys. G: Nucl. Part. Phys. 44 (2017) 064005.
[30] N. Nakatsuka, et al., Phys. Lett. B 768 (2017) 387.
[31] http://cern.ch/geant4.
[32] F. Quarati, et al., Nucl. Instrum. Methods A 683 (2012) 46.
[33] A. Camp, et al., Appl. Rad. Isot. 109 (2016) 512.
[34] A. Giaz, et al., Europhys. Lett. 110 (2015) 42002.
[35] W. Wolszczak, P. Dorenbos, Nucl. Instrum. Methods A 857 (2017) 66.
[36] I. Mazumdar, et al., Nucl. Instrum. Methods A 201 (2010) 995.
[37] M. Ciemala, et al., Nucl. Instrum. Methods A 608 (2009) 76.
[38] F. Quarati, et al., Nucl. Instrum. Methods A 629 (2011) 157.
[39] A. Kafkarkou, et al., Phys. Rev. C 89 (2014) 014601.
[40] S. Chauvie, et al., IEEE Nucl. Sci. Conf. Rec. 3 (2004) 1881.
[41] A. Lechner, M.G. Pia, M. Sudhakar, IEEE Trans. Nucl. Sci. NS-56 (2009) 398.
[42] S. Hauf, et al., IEEE Trans. Nucl. Sci. NS-60 (2013) 2984.